Resonant diffraction radiation from an ultrarelativistic particle moving close to a tilted grating

A. P. Potylitsyn, P. V. Karataev,* and G. A. Naumenko
Institute for Nuclear Physics, Tomsk Polytechnic University, 634050, prospekt Lenina 2A, Tomsk, Russia
(Received 5 August 1999)

A simple model for calculating the diffraction radiation characteristics from an ultrarelativistic charged particle moving close to a tilted ideally conducting strip is developed. Resonant diffraction radiation (RDR) is treated as a superposition of the radiation fields for periodically spaced strips. The RDR characteristics have been calculated as a function of the number of grating elements, tilted angle, and initial particle energy. An analogy with both the resonant transition radiation in an absorbing medium and the parametric x-ray radiation is noted.

PACS number(s): 41.60.−m

I. INTRODUCTION

To date, a number of different approaches [1–4] have been employed to treat the characteristics of electromagnetic radiation from a relativistic particle moving parallel to and above a diffraction grating [the so-called Smith-Purcell effect (SPE)]. The interest in this type of radiation is related both to the possibility of using the SPE to generate intense radiation in the millimeter and submillimeter regions [5] and to implementing it in nondestructive beam diagnostics [6]. In both cases we have to estimate the influence of such factors as transverse beam size, angular beam divergence, monochromaticity, etc., on the radiation characteristics.

In principle, the beam divergence effects in a plane that is parallel to the grating can be estimated using the results obtained in [4]. However, there is no simple algorithm to calculate the radiation characteristics from a particle passing above a tilted grating, i.e., for a nonzero angle between the particle trajectory and the main plane of the grating.

One of the authors of the present paper has developed an approach based on description of the SPE as a resonant diffraction radiation (RDR) [2], which is suitable for calculating the radiation characteristics for a grating consisting of a number of conducting strips spaced by vacuum gaps. Here, we calculate the RDR characteristics of a particle whose trajectory is not parallel to the grating. The influence of geometry on the RDR characteristics is also studied.

II. DIFFRACTION RADIATION FROM AN ULTRARELATIVISTIC PARTICLE FOR A TILTED STRIP

To calculate the RDR characteristics for a tilted grating it is necessary to know the diffraction radiation field from a charged particle moving close to a single tilted strip. The exact solution of the Maxwell equations describing the radiation from a charged particle moving above an inclined semi-infinite ideally conducting screen has long been known [7]. Using the latter and the results reported in [8], we can obtain an expression for the diffraction radiation (DR) field strength for a tilted strip as the difference between the radiation fields of two semi-infinite planes, one restricted by edge 1 and the other by edge 2 (see Fig. 1),

$$\vec{E}_{strip}=\vec{E}_{up}-\vec{E}_{down}\,. \tag{1}$$

For convenience, we express the impact parameter (the shortest distance between the particle trajectory and the plane edge) for edge 1 in the following way:

$$a_1=h-\frac{a}{2}\sin\Theta_0, \tag{2}$$

and for edge 2,

$$a_1=h+\frac{a}{2}\sin\Theta_0. \tag{3}$$

Here h is the spacing between the particle trajectory and the middle line of the strip, a is the strip width, and Θ_0 is the strip tilt angle. Thus, taking into account the phase shift we have

$$\vec{E}_{strip}=\vec{E}_{DR}\left(h-\frac{a}{2}\sin\Theta_0\right)e^{i\phi}-\vec{E}_{DR}\left(h+\frac{a}{2}\sin\Theta_0\right)e^{-i\phi}. \tag{4}$$

In Eq. (4) the DR field for a semi-infinite ideal screen is expressed through $\vec{E}_{DR}(a_i)$. The full phase shift (2ϕ) characterizes the phase difference between the waves being formed in the vicinity of edges 1 and 2 [9]; and it can be derived from simple geometrical relations as a quantity which is proportional to the time difference between the wave propagation from edge 1 and edge 2 (see Fig. 1),

$$2\phi=\frac{2a\pi[\cos(\Theta_y-\Theta_0)-\cos\Theta_0/\beta]}{\lambda}, \tag{5}$$

where β is the particle velocity and λ is the DR wavelength. (In this paper use is made of the system of units $h=m=c=1$.) For the extreme cases ($\Theta_0=0°$ and 90°), the phase shift calculated according to Eq. (5) coincides with that obtained in [2].

Equation (4) is valid if the following conditions for the strip dimensions are fulfilled: $\gamma\lambda>>b$, $\gamma\lambda<<c$ (see Fig. 1). Here γ is the Lorentz factor of the particle.

*Author to whom correspondence should be addressed. Electronic address: kpv@npi.tpu.ru

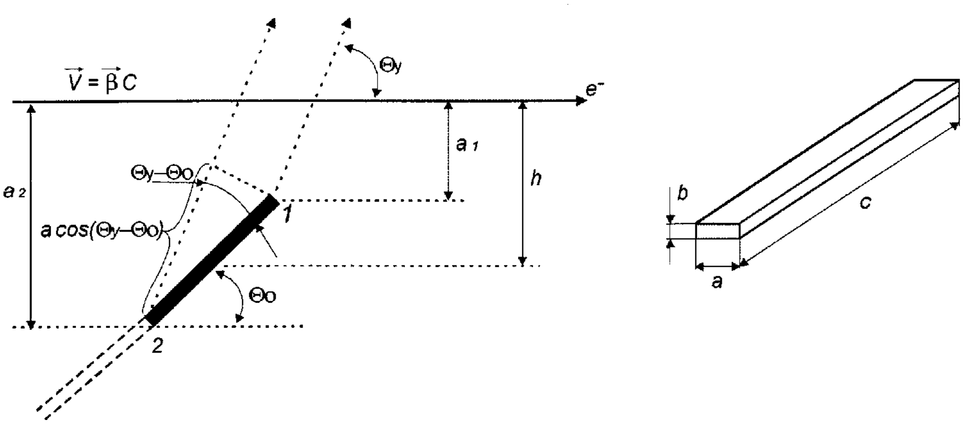

FIG. 1. Geometry of diffraction radiation from a single strip; h is the impact parameter, Θ_y is the observation angle, Θ_0 is the strip tilt angle, and a is the strip width.

We will consider the radiation characteristics in a coordinate system where the z axis is directed along the beam and the x axis is parallel to and the y axis perpendicular to the strip edge. As shown in [8], for relativistic particles the radiation concentrates in the range of angles

$$|\Theta_x| \leqslant \gamma^{-1} \tag{6}$$

if $\gamma >> 1$. In this approximation the following expression for the DR yield with wavelength λ will be true:

$$\vec{E}_{DR}(x+\Delta x) = \vec{E}_{DR}(x)\exp\left(-\frac{2\pi\Delta x}{\gamma\lambda}\sqrt{1+\gamma^2\Theta_x^2}\right), \tag{7}$$

where $\vec{E}_{DR}(x) \sim \exp[-(\omega/2\omega_c)\sqrt{1+\gamma^2\Theta_x^2}]$, and $\omega_c = \gamma/2a_1$ is the DR characteristic energy.

For further calculations we shall use a more symmetrical expression instead of Eq. (4):

$$\vec{E}_{strip} = \vec{E}_{DR}(h)[\exp(\alpha+i\phi) - \exp(-\alpha-i\phi)], \tag{8}$$

$$\alpha = \left(\frac{a\pi\sin\Theta_0}{\gamma\lambda}\right)\sqrt{1+\gamma^2\Theta_x^2}. \tag{9}$$

From Eq. (8) we derive the following fomula for the DR spectral-angular density for the strip:

$$\frac{d^2W_{strip}}{d\omega\, d\Omega} = \frac{d^2W_{DR}}{d\omega\, d\Omega}F_{strip}, \tag{10}$$

$$\frac{d^2W_{DR}}{d\omega\, d\Omega} = 4\pi^2|\vec{E}_{DR}|^2, \quad F_{strip} = 4(\sinh^2\alpha + \sin^2\phi). \tag{11}$$

The expressions obtained are quite similar to the formulas for the spectral-angular distribution of transition radiation (TR) from a foil (see, e.g., [10]). In the case in question, F_{strip} characterizes the DR field interference from the two strip edges; whereas, for TR, the same multiplier characterizes the TR field interference from the input and output surfaces of the foil.

Earlier [9], the spectral-angular density of DR for a semi-infinite screen was obtained using an ultrarelativistic approximation. It was shown that the DR is concentrated in the vicinity of the plane that is perpendicular to the screen ($\Theta_x \sim \gamma^{-1}$),

$$\frac{d^2W_{DR}}{d\omega\, d\Omega} = \frac{\alpha}{4\pi^2}\exp[-(\omega/\omega_c)\sqrt{1+\gamma^2\Theta_x^2}]$$
$$\times\{\Theta_x^2[1+\cos(\Theta_y-\Theta_0)](1-\cos\Theta_0)$$
$$+(\gamma^{-2}+\Theta_x^2)[1-\cos(\Theta_y-\Theta_0)]$$
$$\times(1+\cos\Theta_0)\}((\gamma^{-2}+\Theta_x^2)\{[\cos(\Theta_y-\Theta_0)$$
$$-\cos\Theta_0/\beta]^2+(\gamma^{-2}+\Theta_x^2)\sin^2\Theta_0\})^{-1}. \tag{12}$$

In Eq. (12), we have omitted the terms smaller than $\sim\gamma^{-2}$ in the numerator and denominator.

Now we shall consider the forward diffraction radiation (FDR), i.e., for the angles $\Theta_y \sim \gamma^{-1} \ll 1$. Using this approximation instead of Eq. (12) we have

$$\frac{d^2W_{DR}}{d\omega\, d\Omega} = \frac{\alpha}{4\pi^2}\exp\left(-\frac{\omega}{\omega_c}\sqrt{1+\gamma^2\Theta_x^2}\right)$$
$$\times\frac{\gamma^{-2}+2\Theta_x^2}{(\gamma^{-2}+\Theta_x^2)(\gamma^{-2}+\Theta_x^2+\Theta_y^2)}. \tag{13}$$

As was noted in [8], in the angular distribution of DR at $\Theta_y = \Theta_x = 0$ there is a maximum whose value is proportional to γ^2,

$$\frac{d^2W_{DR}(\Theta_x=0,\Theta_y=0)}{d\omega\, d\Omega} = \frac{\alpha}{4\pi^2}\gamma^2\exp\left(-\frac{\omega}{\omega_c}\right). \tag{14}$$

For $\Theta_y \gg \gamma^{-1}$, using Eq. (12) one can obtain a simpler expression:

$$\frac{d^2W_{DR}}{d\omega\, d\Omega} = \frac{\alpha}{4\pi^2}\exp[-(\omega/\omega_c)\sqrt{1+\gamma^2\Theta_x^2}]\{\gamma^{-2}(1+\cos\Theta_0)$$
$$\times[1-\cos(\Theta_y-\Theta_0)]+2\Theta_x^2[1-\cos\Theta_0$$
$$\times\cos(\Theta_y-\Theta_0)]\}[(\gamma^{-2}+\Theta_x^2)\sin^2(\Theta_y/2)$$
$$\times\sin^2(\Theta_0-\Theta_y/2)]^{-1}. \tag{15}$$

It follows from Eq. (12) that for the mirror reflection angle ($\Theta_y = 2\Theta_0$) the angular distribution has another maximum which is much the same as Eq. (14) and can be identified as ''backward diffraction radiation'' (BDR) in analogy with the process of transition radiation. The fact that the FDR and BDR intensities coincide in the whole frequency range re-

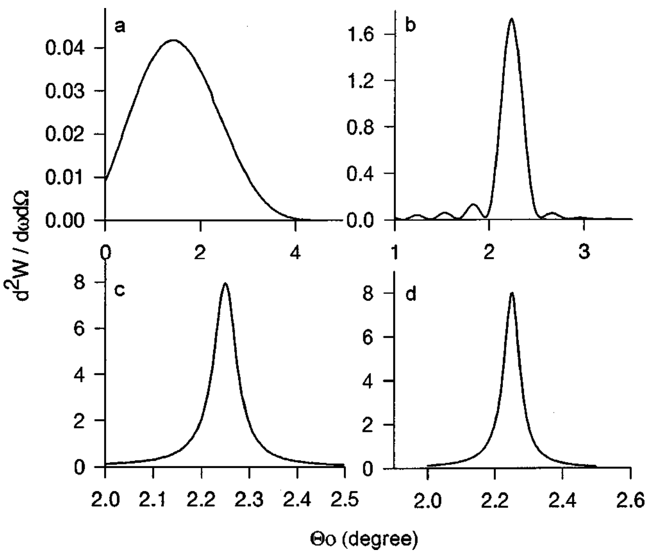

FIG. 2. Orientation dependence for a single strip with the widths $a=0.1$ mm (a), 1 mm (b), 10 mm (c), and a semi-infinite plane (d).

sults from using an ideally conducting screen approximation. However, it is obvious that the latter approximation is not valid for $\omega_c \gg \omega_p$, where ω_p is the plasmon energy of the screen material.

In the range of angles $|2\Theta_0-\Theta_y|\sim\gamma^{-1}$, i.e., in the vicinity of the mirror reflection direction, the BDR spectral-angular density also has the form of Eq. (13); however, in this case the angle Θ_y is measured from the mirror reflection direction (see [8]).

Thus, Eq. (15) is valid when the following conditions are fulfilled:

$$\Theta_y \gg \gamma^{-1}, \quad |2\Theta_0-\Theta_y| \gg \gamma^{-1}. \tag{16}$$

In this case, as follows from Eq. (15), the DR density is about γ^2 times smaller.

Figure 2 shows the dependence of the DR yield on the strip tilt angle Θ_0 (the so-called orientation dependence) for the fixed observation angle $\Theta_y=4.5°$ in the reflection plane $(\Theta_x=0)$. The calculations have been carried out using Eqs. (10)–(12) for $\gamma=1000$, $\lambda=0.4$ μm, and $a_1=0.1$ mm. One can see that for $\gamma\lambda \gg a\sin\Theta_0$ the DR yield is strongly suppressed and the characteristic angular width of the dependence is significantly higher than $\sim\gamma^{-1}$, which is typical for DR from a semi-infinite screen [see Fig. 2(d)]. The DR intensity at the orientation dependence maximum is also suppressed when $\gamma\lambda \gg a\sin\Theta_0$.

III. RESONANT DIFFRACTION RADIATION FROM A TILTED GRATING

Let us consider a grating consisting of N strips of width a and period d tilted at angle Θ_0 to the electron momentum (see Fig. 3). The impact parameter [the distance between the first strip center and the electron trajectory (see Fig. 1)] we denote as h.

The radiation field being formed near strip 1 of the grating coincides with Eq. (8),

$$\vec{E}_1=\vec{E}_{strip}(h), \tag{17}$$

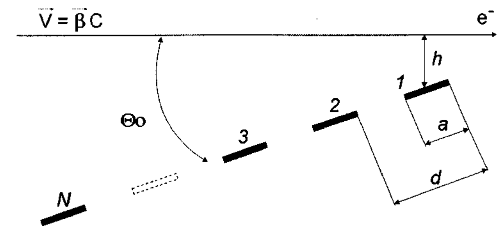

FIG. 3. Geometry of diffraction radiation from a tilted grating; h is the impact parameter, a is the strip width, d is the grating period, and Θ_0 is the grating tilt angle.

whereas the next strip field differs from Eq. (17) in both the phase ϕ_0 and the decay factor α_0,

$$\vec{E}_2=\vec{E}_1\exp(-\alpha_0-i\phi_0)=\vec{E}_{strip}(h)\exp(-\alpha_0-i\phi_0), \tag{18}$$

which can be determined in analogy to Eqs. (5) and (9):

$$\phi_0=\frac{2\pi d[\cos(\Theta_y-\Theta_0)-\cos\Theta_0/\beta]}{\lambda}, \tag{19}$$

$$\alpha_0=\left(\frac{2\pi d\sin\Theta_0}{\gamma\lambda}\right)\sqrt{1+\gamma^2\Theta_x^2}. \tag{20}$$

One can write the kth strip field in the same way,

$$\vec{E}_k=\vec{E}_{strip}\exp[-(k-1)(\alpha_0+i\phi_0)]. \tag{21}$$

The resulting field of the N strip grating is expressed through the sum of N terms

$$\vec{E}_{GR}=\vec{E}_1+\vec{E}_2+\cdots+\vec{E}_k =\vec{E}_{strip}\sum_{k=1}^{N}\exp[-(k-1)(\alpha_0+i\phi_0)]. \tag{22}$$

Having calculated the squared modulus of Eq. (22) we obtain the following expression for the DR spectral-angular density for the entire grating:

$$\frac{d^2W_{GR}}{d\omega\,d\Omega}=\frac{d^2W_{strip}}{d\omega\,d\Omega}F_N=\frac{d^2W_{DR}}{d\omega\,d\Omega}F_{strip}F_N, \tag{23}$$

where

$$F_N=\left|\sum_{k=1}^{N}\exp[-(k-1)(\alpha_0+i\phi_0)]\right|^2=\left|\frac{1-C^N}{1-C}\right|^2. \tag{24}$$

Here $C=\exp(-\alpha_0-i\phi_0)$.

After simple mathematical transformations, Eq. (24) may be written in the following manner:

$$F_N=\exp[-(N-1)\alpha_0]\left(\frac{\sin^2(N\phi_0/2)+\sinh^2(N\alpha_0/2)}{\sin^2(\phi_0/2)+\sinh^2(\alpha_0/2)}\right). \tag{25}$$

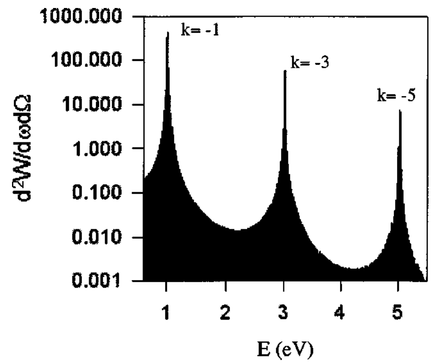

FIG. 4. Smith-Purcell effect spectrum. The initial conditions used are $\Theta_y = 4.5°$, $\Theta_x = 0$, $\Theta_0 = 0$, $a = 0.2$ mm, $d = 0.4$ mm, $h = 0.1$ mm, $\gamma = 1000$, $N = 50$; k is the diffraction order.

One should notice that the structure of Eq. (25) is identical to that of a similar expression for the resonant transition radiation from N layers taking into account the radiation absorption in every layer.

First we shall consider a particular case corresponding to the Smith-Purcell geometry $(\Theta_0 = 0)$. It is obvious that the decay factor α_0 determined by Eq. (20) is equal to zero, so that Eq. (25) can be rewritten in a well-known form:

$$F_N = \frac{\sin^2(N\phi_0/2)}{\sin^2(\phi_0/2)}. \tag{26}$$

When $N \to \infty$, Eq. (26) transforms into an ordinary δ function,

$$F_N = 2\pi N \delta(\phi_0 - 2k\pi), \tag{27}$$

where k is the diffraction order.

The presence of the δ function is an indication of the existence of monochromatic maxima in the RDR spectrum. However, the use of the δ function for real gratings where the number of elements is limited is not always justified. Therefore, we shall further use the exact formulas (25) and (26).

Figure 4 depicts the RDR spectral distribution for the Smith-Purcell geometry. The calculation has been carried out for $a = d/2$ when the intensity reaches its maximum value [2]. The peak position in the spectrum is determined by the phase relation (the resonance condition)

$$\phi_0 = 2k\pi, \tag{28}$$

which leads to the well-known formula of Smith-Purcell,

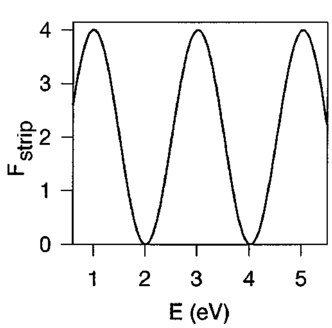

FIG. 5. Dependence of F_{strip} on energy.

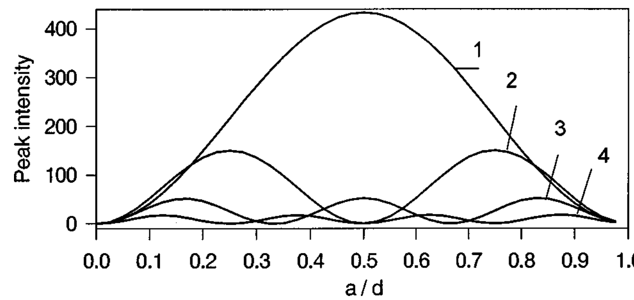

FIG. 6. Dependence of the first (1), second (2), third (3), and fourth (4) order maximum intensity on the ratio a/d. The initial conditions used are $\Theta_y = 4.5°$, $\Theta_x = 0$, $\Theta_0 = 0$, $h = 0.1$ mm, $\gamma = 1000$, $N = 50$, $\lambda = 0.4$ μm.

$$\lambda_k = \frac{d(\cos\Theta_y - 1/\beta)}{k}. \tag{29}$$

As is seen from the figure, the even orders are absent. This is explained by the influence of the F_{strip} factor, which is equal to zero at

$$\phi = m\pi, \tag{30}$$

where m is on integer [see Eq. (11)].

Substituting Eq. (29) in Eq. (5), we can write Eq. (28) in the following form:

$$k = \frac{d}{a} m = 2m. \tag{31}$$

Thus, in the case under consideration $(a = d/2)$ the even diffraction orders are forbidden. For illustration, Fig. 5 shows the dependence of F_{strip} on the photon energy calculated for the same conditions as in Fig. 4.

Figure 6 shows the maximum DR yield dependence on the ratio a/d for four radiation orders. As was shown above, for the first diffraction order the intensity reaches its maximum value at $a/d = 0.5$, and for the second order at $a/d = 0.25$ and 0.75.

Let us consider the case of a tilted grating. One should note that in the DR spectrum quasimonochromatic peaks can be observed at small tilt angles of the grating. For the tilted

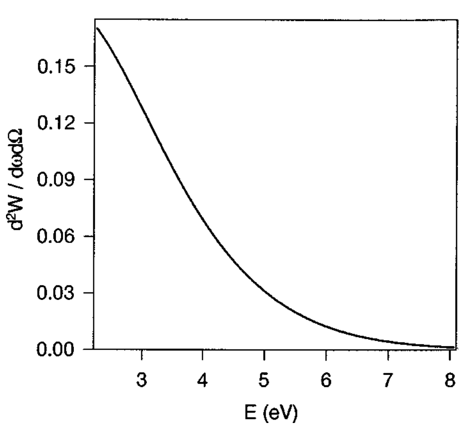

FIG. 7. Diffraction radiation spectrum from a tilted strip. The initial conditions used are $\Theta_y = 4.5°$, $\Theta_x = 0$, $\Theta_0 = 1.9°$, $a = 0.2$ mm, $a_1 = 0.1$ mm (see Fig. 1), $\gamma = 1000$.

single strip the spectrum calculated according to Eq. (10) is shown in Fig. 7. The strip parameters and geometry are indicated in the figure caption. As in the case of a semi-infinite screen one can observe an exponentially decreasing spectrum.

Figure 8 depicts the RDR spectrum from a tilted grating calculated at $\Theta_0=1.9°$. Unlike the spectrum from a single strip calculated for the same initial conditions, here one can observe a first order quasimonochromatic radiation maximum with a finite full width at half maximum (FWHM) together with a continuous background.

The positions of the quasimonochromatic maxima in the RDR spectrum are determined by the resonance condition (28) where the ϕ_0 phase is taken according to Eq. (19). We will illustrate this fact in the following way. Let us rewrite Eq. (25) in the form

$$F_N=\frac{1-2\exp[-(N-1)\alpha_0]\cos[(N-1)\phi_0]+\exp[-2(N-1)\alpha_0]}{1-2\exp(-\alpha_0)\cos\phi_0+\exp(-2\alpha_0)}. \tag{32}$$

In the extreme case, when $N\rightarrow\infty$, instead of Eq. (32) we have

$$F_\infty=\frac{1}{1-2e^{-\alpha_0}\cos\phi_0+e^{-2\alpha_0}}. \tag{33}$$

It is apparent that the expression obtained reaches its maximum value when the following conditions are fulfilled:

$$\phi_0=2k\pi \quad (\cos\phi_0=1). \tag{34}$$

In this case,

$$F_\infty=\frac{1}{(1-e^{-\alpha_0})^2}. \tag{35}$$

At small values $\alpha_0 \ll 1$, which correspond to small tilt angles of the grating, $\Theta_0 \ll 1$, from Eq. (35) we have

$$F_\infty\cong\frac{1}{\alpha_0^2}. \tag{36}$$

Thus, pronounced quasimonochromatic maxima in the DR spectrum can be observed at grazing incidence angles of the particle beam with respect to the grating. For the angle $\Theta_0 \neq 0$, instead of the Smith-Purcell conditions we have the following relation between the quasimonochromatic maximum position, period d, grating tilt angle Θ_0, and observation angle Θ_y:

$$\lambda_k=\frac{d[\cos(\Theta_y-\Theta_0)-\cos\Theta_0/\beta]}{k}, \tag{37}$$

where k is an integer.

Figure 9(a) shows the dependence of different-order maximum positions on the target orientation angle at the observation angle $\Theta_y=4.5°$. One can see that for negative values of Θ_0 (i.e., for the geometry where the beam ''reflected'' by the grating is directed to the opposite side from the detector) the spectral maxima are shifted to low energy with respect to the SPE spectrum ($\Theta_0=0$). When the tilt angle increases, the spectral maxima are shifted to the high energy part.

A similar peak shift of the parametric x-ray radiation (PXR) has been registered in an experiment [11] with a rotating crystalline target. Actually, for both RDR and PXR the peak position in the spectrum is determined by the resonance condition only and does not depend on the radiation mechanism.

The PXR studies often measure a so-called θ–scan, i.e., the dependence of the radiation yield for a fixed observation angle and electron energy on the target orientation angle. Figure 9(b) presents this dependence calculated for the RDR. In this case the grating tilt angle Θ_0 is varied with respect to the electron beam.

A recent experiment [12] measured the same dependence for the Smith-Purcell effect for a grating made as a periodically deformed continuous surface. The authors of that paper obtained a dependence with clear maxima. This dependence shape is quite close to the one presented in Fig. 9(b).

Figure 10(a) presents the dependence of the full width at half maximum (ΔE) on the number of grating elements for the first diffraction order and tilt angle $\Theta_0=1°$ (solid line). It also shows a similar dependence for the SPE, which is well approximated by a $1/N$ dependence (dotted line). As follows from the figure, for $\Theta_0=1°$ the resulting curve is well approximated by the C_1/N formula where $C_1=1.8$. When the number of periods increases, the RDR intensity also increases, reaching the $0.95I_\infty$ level for $N=70$ [see Fig. 10(b)].

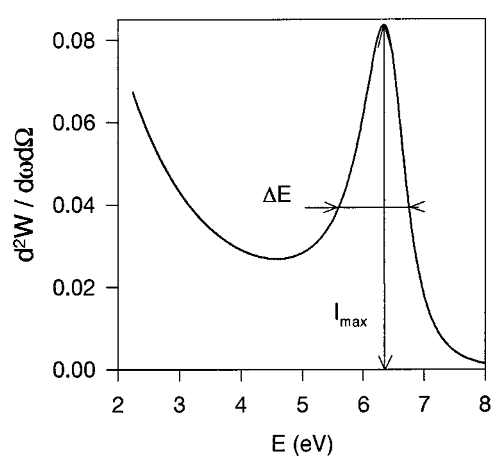

FIG. 8. Diffraction radiation spectrum from a tilted grating. The initial conditions used are $\Theta_y=4.5°$, $\Theta_x=0$, $\Theta_0=1.9°$, $a=0.2$ mm, $h=0.1$ mm (see Fig. 3), $\gamma=1000$.

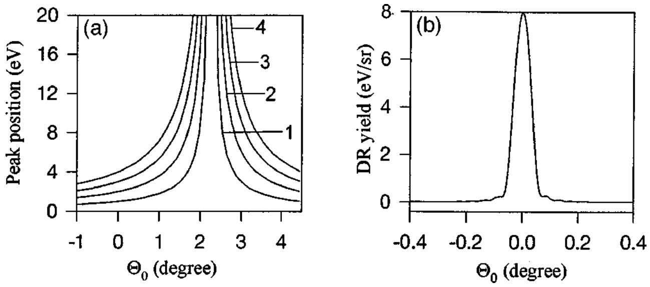

FIG. 9. (a) Dependence of the first (1), second (2), third (3), and fourth (4) order peak positions ($\Theta_y = 4.5°$, $d = 0.4$ mm) on the tilt angle. (b) Dependence of the first DR order yield ($\lambda = 1233$ nm) on the tilt angle.

Let us estimate the effective grating length (the number of periods) with which the passing particle field interacts:

$$N_{eff} = \frac{\gamma\lambda}{d \sin\Theta_0}. \tag{38}$$

In the case considered, $N_{eff} = 60$, which is quite close to the grating length, providing a 95% intensity level.

When a particle moves close to a grating of limited length (with the number of periods N), one can derive a similar characteristic for the Lorentz factor:

$$\gamma_{eff} = N \frac{d \sin\Theta_0}{\lambda}. \tag{39}$$

Figure 11 shows the dependence of I_{max} on the particle energy. As follows from the figure the simple estimation (39) is a good characteristic for the RDR process too.

IV. SUMMARY

A simple model for calculating the RDR characteristics from a tilted grating has been suggested. It has been shown that quasimonochromatic maxima appear in the RDR spectrum, and their characteristics (full width, intensity) are determined primarily by the angle between the grating plane and electron pulse.

Let us estimate the initial beam divergence effect for the SP geometry. It was noticed in [4] that for angles $\Theta_H \ll 1$ (Θ_H is the angle between the electron momentum and grating axis in the horizontal plane) the peak shift can be described in the following way:

$$\lambda_k = \frac{d}{\cos\Theta_H} \frac{\cos\Theta_y - 1/\beta}{k} \simeq \lambda_k^0 \left(1 + \frac{\Theta_H^2}{2}\right). \tag{40}$$

Thus,

$$\frac{\Delta\lambda_H}{\lambda} = \frac{\Theta_H^2}{2}, \tag{41}$$

and therefore the peak broadening related to beam divergence in horizontal plane can be neglected if

$$\frac{\Theta_H^2}{2} \ll \frac{1}{N}, \tag{42}$$

which is generally fulfilled.

In order to obtain a formula analogous to Eq. (41) and characterizing the beam broadening due to the divergence in the vertical plane, we shall take into account that the observation angle

$$\Theta_y - \Theta_0 = \Theta_D = \text{const}, \tag{43}$$

where the angle Θ_D is measured from the grating plane. Let us denote the angle Θ_0 as Θ_V (Θ_V is the angle between the electron pulse and grating axis in the vertical plane). Then for $\Theta_V \ll 1$ we have

$$\lambda_k = \frac{d}{k}\left(\cos\Theta_D - \frac{1 - \Theta_V^2/2}{\beta}\right). \tag{44}$$

It follows from Eq. (44) that the SPE peak broadening is determined by the observation angle Θ_D:

$$\frac{\Delta\lambda_V}{\lambda} \simeq -\frac{\Theta_V^2}{4\sin^2(\Theta_D/2)}. \tag{45}$$

For small observation angles Θ_D the peak broadening $\Delta\lambda_V/\lambda$ can be significant and exceed the ''natural'' peak

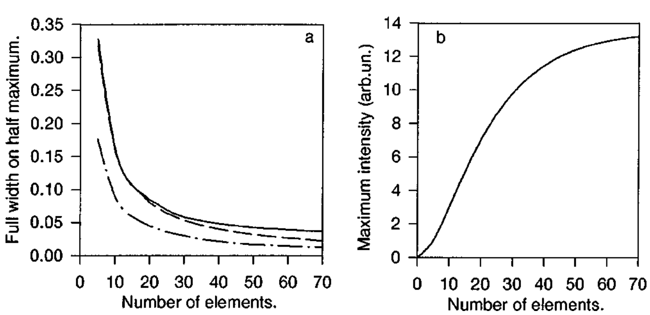

FIG. 10. (a) Dependence of the first order FWHM for the SPE for ($\Theta_0 = 0$) (solid line) and $\Theta_0 = 1°$ (dash-dotted line) on the number of elements, and dependence on $1/N$ (dashed line). The initial conditions used are $\Theta_y = 4.5°$, $\Theta_x = 0$, $a = 0.2$ mm, $h = 0.1$ mm, $d = 0.4$ mm (see Fig. 1), $\gamma = 1000$. (b) Dependence of the first order maximum intensity on the number of elements calculated for the same initial conditions.

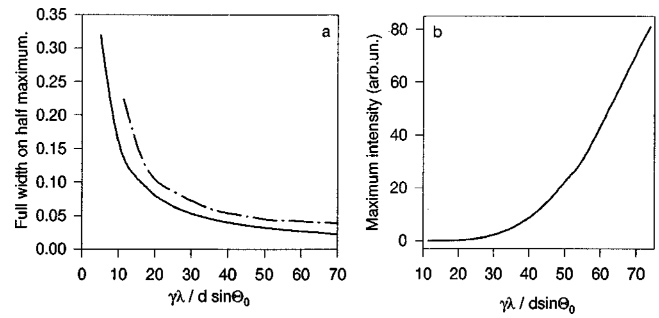

FIG. 11. (a) Dependence of the first order FWHM (dash-dotted line) on N_{eff} and the $1/N_{eff}$ function (solid line). The initial conditions used are $\Theta_y = 4.5°$, $\Theta_x = 0$, $\Theta_0 = 1°$, $a = 0.2$ mm, $h = 0.1$ mm, $d = 0.4$ mm (see Fig. 1), $\gamma = 1000$. (b) Dependence of the first order maximum intensity on N_{eff} calculated for the same initial conditions.

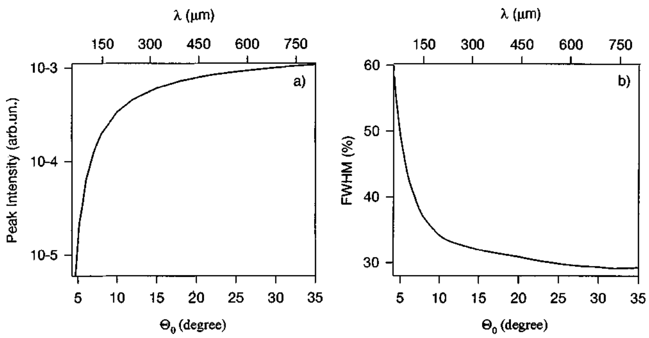

FIG. 12. (a) Dependences of the RDR peak intensity on the grating tilt angle (radiation wavelength) for $\gamma=100$, $\Theta_y=4.5°$, $d=20$ mm, $a=10$ mm. (b) Dependence of the FWHM on the grating tilt angle (radiation wavelength) for the same initial conditions.

width $1/N$. Thus, by changing the SPR peak width for small angles Θ_D, in principle, one can determine the vertical beam divergence.

From Eq. (45) one can estimate the sensitivity of the method:

$$\Theta_V \geqslant \frac{2\sin(\Theta_D/2)}{\sqrt{N}}. \tag{46}$$

Since this expression does not depend on the wavelength, investigation of the line shape can be carried out in the optical region. For example, for $\Theta_D=2°$ and $N=100$, $\Theta_V \sim 3.5\times10^{-3}$. The estimation obtained does not depend on γ (if $\gamma \gg 1$).

The technique suggested for beam divergence determination can be used in accelerators with $\gamma \leqslant 100$, because, in this case, the well-known methods based on either transition radiation or synchrotron radiation exhibit a sensitivity controlled by the characteristic radiation angle γ^{-1}.

The dependence of the peak position in the RDR spectrum on the grating tilt angle Θ_0 can be used to determine the electron bunch length l_e. In [6,13] the authors suggested measuring the coherent SPR yield at different observation angles. In the wavelength region of $\lambda \sim l_e$ one will observe conversion from ordinary SPR to coherent SPR, i.e., the radiation intensity will be changed by approximately N_e times (N_e is the number of electrons in a bunch).

Figure 12(a) shows the dependence of the RDR wavelength on the grating tilt angle for the fixed observation angle Θ_y, and a similar dependence for the peak width is presented in Fig. 12(b). The calculations have been carried out for the following conditions:

$$\gamma=100, \quad \Theta_y=4.5°, \quad d=20 \text{ mm}, \quad a=10 \text{ mm}.$$

As follows from the figure, in the wavelength region $\lambda=0.15$–0.8 mm ($\Theta_0=8°$–$35°$) an almost constant intensity of the ordinary RDR is observed. If we measure the RDR intensity for an electron bunch with the length $l_e \sim 0.5$ mm, then for the grating tilt angles indicated one could research the conversion to the ''coherent RDR mode'' in detail, which would allow one to determine both the average bunch length and the profile of electron distribution in a bunch. The technique suggested is related to grating rotation for a fixed detector position, whereas in [6,13] it was sugested to move the detector, which is not always convenient (in particular, if the detecting system contains a monochromator).

Depending on the bunch length l_e, the region of the wavelengths investigated can be easily changed by choosing a proper grating period and observation angle.

ACKNOWLEDGMENT

This work was carried out with partial support by the Russian Basic Research Fund (Grant Nos. 98-02-17994 and 99-02-16884).

[1] O. Haeberle *et al.*, Phys. Rev. E **49**, 3340 (1994).
[2] A.P. Potylitsyn, Phys. Lett. A **238**, 112 (1998).
[3] K.J. Woods *et al.*, Phys. Rev. Lett. **74**, 3808 (1995).
[4] O. Haeberle *et al.*, Phys. Rev. E **55**, 4675 (1997).
[5] Y. Shibata *et al.*, Phys. Rev. E **52**, 6787 (1995).
[6] M.C. Lampel, Nucl. Instrum. Methods Phys. Res. A **385**, 19 (1997).
[7] A.P. Kazantsev and G.I. Surdutovich, Dokl. Akad. Nauk USSR **147**, 74 (1963) [Sov. Phys. Dokl. **7**, 990 (1963)].
[8] A.P. Potylitsyn, Nucl. Instrum. Methods Phys. Res. B **145**, 169 (1998).
[9] A.P. Potylitsyn, Nucl. Instrum. Methods Phys. Res. B **145**, 60 (1998).
[10] X. Artru, G.B. Yodh, and G. Mennessier, Phys. Rev. D **12**, 1289 (1975).
[11] Yu.N. Adishev *et al.*, Nucl. Instrum. Methods Phys. Res. B **44**, 130 (1989).
[12] G. Kube *et al.*, Ph.D. Dissertation, Mainz Microtron MAMI, Mainz, Germany, 1998 (unpublished).
[13] Dinh C. Nguyen, Nucl. Instrum. Methods Phys. Res. A **393**, 514 (1997).